Application of FEM-BIE for Scattering from Dielectric Objects Buried under a Rough Surface

Runwen Xu*, and Lixin Guo

School of Physics and Optoelectronic Engineering, Xidian University, Xi'an, China (e-mail: rwxu719@126.com)

Abstract

This paper presents a hybrid method combining the finite element method (FEM) with the boundary integral equation (BIE) for two dimensional (2D) scattering from dielectric objects buried under the rough surface. In the hybrid method, one boundary integral equation is adopt to depict the scattering above the rough surface on the basis of Green's function. Based on the domain decomposition technique, the computational region below the rough ground is divided into multiple isolated interior regions containing each object and the exterior region. Finite element formulations are only applied inside interior regions to derive a set of linear systems, and another boundary integral formula is developed below the rough surface which also act as the boundary constraints of the FEM regions. Compared with traditional FEM based on perfectly matched layer (PML), the hybrid technique presented here is highly efficient in terms of computational memory, time, and versatility.

1. Introduction

The finite element method (FEM) is used extensively to perform electromagnetic modeling, because it is efficient in modeling the scattering geometries which are both penetrable and inhomogeneous. In the application of FEM, the approximate absorbing boundaries, such as the absorbing boundary conditions (ABC) [1, 2] and perfectly matched layer (PML) [3, 4], are usually used as the constrained boundary. However, the approximate absorbing boundaries often need to be set far enough away from the model surface to keep their precision, and are often invalid to some particular problems. To improve the precision and the versatile of FEM, the boundary integral equation [5, 6] is introduce as the artificial truncated boundary. The earlier work based on FEM always used an artificial boundary to enclose the whole scattering model, which consumes largely of computational time and memory. In this paper, a hybrid method combining FEM with boundary integral equation (FEM-BIE) is extended to the simulations of the scattering from dielectric objects buried beneath the rough surface. Here, FEM is applied only inside the interior regions, while another boundary integral equation is applied in the exterior region. On the artificial boundaries between the interior region and the exterior region, the equations of different domains are coupled by the continuous boundary conditions. The hybrid algorithm presented here shows effectiveness and efficiency in terms of computing resources, computational time, and versatile applications.

2. Theoretical analysis

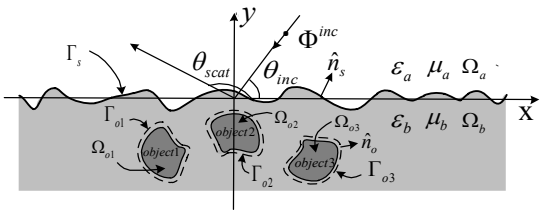

Figure 1. The 2D scattering problem of multiple objects buried beneath the rough ground

Figure 1 shows multiple objects with an arbitrary shape are buried under the dielectric rough surface. Φ^{inc} represent the incident wave, which impinges on the composite model with a incidence angle θ_{inc} and is scatted with a scattering angle θ_{scat}. The symbol $\hat{n}$ is the unit normal vector on the artificial boundaries. Γ_o are the boundaries of the objects, while Γ_s denotes the truncated part of the rough surface. The interior region Ω_{in} is defined as the region of the objects, and each subdomain of Ω_{in} is expressed by Ω_o. Ω_a and Ω_b shows the region above the rough surface and the region below the rough surface, respectively. For the region Ω_o of each dielectric object, the boundary Γ_o is also applied as the truncated boundary of FEM region.

978-1-4673-5225-3/14/$31.00 ©2014 IEEE

The incident wave $\boldsymbol{E}^{inc}$ is assumed to be invariant along the z axis, and therefore the electric field of the wave only has the component of E_z denoted by Φ. Above the rough surface, the electric field satisfied the Helmholtz equation (a time factor $e^{j\omega t}$ has been assumed and suppressed), which can be written as

$$\nabla^2\Phi(\boldsymbol{r})+k_a^2\Phi(\boldsymbol{r})=f(\boldsymbol{r}) \tag{1}$$

where $\Phi(\boldsymbol{r})$ denotes E_z, k_a is the wavenumber of the space, $f(\boldsymbol{r})$ relates to the current J_z in the space and $f(\boldsymbol{r})=jk_a\eta J_z(\boldsymbol{r})$, η is the characteristic impedance.

Due to the infinite length of the rough surface, it needs to be truncated into a limited length in our simulation. This can introduce the artificial truncated effect at the ends of the rough surface. To reduce this effect, the tapered incident wave is chose as the incident wave which decreases to a very small value at the ends of the rough surface. The form of the incident wave [7] can be expressed as

$$\Phi^{inc}(\boldsymbol{r})=\exp[i\boldsymbol{k}\cdot\boldsymbol{r}(1+w(\boldsymbol{r}))]\cdot\exp\left[-(x-y\cot\theta_{inc})^2/g^2\right] \tag{2}$$

where $w(\boldsymbol{r})=\left[2(x-y\cot\theta_{inc})^2/g^2-1\right]\Big/(kg\sin\theta_{inc})^2$, $\boldsymbol{k}$ is vector of the wavenumber in the space, g is the tapered factor, and $\boldsymbol{r}$ is the position vector.

In domain Ω_a, we introduce the free space Green's function. It satisfies the Sommerfeld radiation condition at infinity and the following differential equation

$$\nabla^2G_a(\boldsymbol{r},\boldsymbol{r}')+k_a^2G_a(\boldsymbol{r},\boldsymbol{r}')=-\delta(\boldsymbol{r}-\boldsymbol{r}') \tag{3}$$

The Green's function of the free space $G_a(\boldsymbol{r},\boldsymbol{r}')$ can be easily found to be the zeroth-order Hankel function of the second kind written as

$$G_a(\boldsymbol{r},\boldsymbol{r}')=\frac{1}{4j}H_0^2(k_a|\boldsymbol{r}-\boldsymbol{r}'|) \tag{4}$$

Multiply Eq. (1) with G_a, integrating over Ω_a, and invoking the second Green's scalar theorem

$$\Phi_{\Gamma_{s+}}(\boldsymbol{r})=\int_{\Gamma_{s+}}\left[\Phi(\boldsymbol{r}')\frac{\partial G_a(\boldsymbol{r},\boldsymbol{r}')}{\partial n_s}-G_a(\boldsymbol{r},\boldsymbol{r}')\frac{\partial\Phi(\boldsymbol{r}')}{\partial n_s}\right]d\Gamma'+\Phi^{inc}(\boldsymbol{r}) \tag{5}$$

where $\Phi^{inc}(\boldsymbol{r})=-\iint_{\Omega_a}\left[G_a(\boldsymbol{r},\boldsymbol{r}')f(\boldsymbol{r}')\right]d\Omega'$, Γ_{s+} is the truncated domain of the rough surface ($+$ denotes the side of the rough surface in domain Ω_a. On the infinite boundary above the rough surface, both $\Phi(\boldsymbol{r})$ and $G_a(\boldsymbol{r},\boldsymbol{r}')$ satisfy the Sommerfeld radiation conditions, while the incident field on the parts of the rough surface which overflow from Γ_S are almost zero due to the adoption of the tapered incident wave. So only the boundary integral on Γ_s remains in Eq. (5).

In the region Ω_b, the Helmholtz equation is still be satisfied

$$\nabla^2\Phi(\boldsymbol{r})+k_b^2\Phi(\boldsymbol{r})=0 \tag{6}$$

where k_b is the wave number of Ω_b. The Green's function $G_b(\boldsymbol{r},\boldsymbol{r}')$ is introduce in region Ω_b, and it also satisfies the Sommerfeld radiation condition at infinity and the following differential equation

$$\nabla^2G_b(\boldsymbol{r},\boldsymbol{r}')+k_b^2G_b(\boldsymbol{r},\boldsymbol{r}')=-\delta(\boldsymbol{r}-\boldsymbol{r}') \tag{7}$$

in which $G_b(\boldsymbol{r},\boldsymbol{r}')$ is the zeroth-order Hankel function of the second kind written as

$$G_b(\boldsymbol{r},\boldsymbol{r}')=\frac{1}{4j}H_0^2(k_b|\boldsymbol{r}-\boldsymbol{r}'|) \tag{8}$$

As the deduction of Eq. (5), the integral equation of Ω_b can be yield as

$$\begin{aligned}\Phi_{\Gamma_{s-.or.oi}}(\boldsymbol{r})=&-\int_{\Gamma_{s-}}\left[\Phi(\boldsymbol{r}')\frac{\partial G_b(\boldsymbol{r},\boldsymbol{r}')}{\partial n_s}-G_b(\boldsymbol{r},\boldsymbol{r}')\frac{\partial\Phi(\boldsymbol{r}')}{\partial n_s}\right]d\Gamma'\\&+\sum_{i=1}^{n}\int_{\Gamma_{oi}}\left[\Phi(\boldsymbol{r}')\frac{\partial G_b(\boldsymbol{r},\boldsymbol{r}')}{\partial n_{oi}}-G_b(\boldsymbol{r},\boldsymbol{r}')\frac{\partial\Phi(\boldsymbol{r}')}{\partial n_{oi}}\right]d\Gamma'\end{aligned} \tag{9}$$

where Γ_{s-} is the truncated domain of the rough surface ($-$ denotes the side of the rough surface in domain Ω_b, and Γ_{oi} is boundaries of the i th subdomain of the object.

On the artificial surfaces of Ω_{in}, the boundary conditions can be assumed as follows for simplification:

$$\frac{1}{\mu_r}\frac{\partial\Phi}{\partial n}\bigg|_{\Gamma}=-\psi \tag{10}$$

As shown in Figure 1, the whole computed space in Ω_b is separated into many isolate interior subdomains. The field in every interior subdomain of the objects can be formulated into an equivalent variational problem [8], whose equivalent variational problem can be given by

$$\delta F_{oi}(\Phi) = 0 \quad i = 1, 2, \cdots, n \tag{11}$$

For every computed subdomain Ω_o, the form of $F(\Phi)$ can be expressed as

$$F_{oi}(\Phi) = \frac{1}{2}\iint_{\Omega_{oi}} [\frac{1}{\mu_r}\left(\frac{\partial \Phi}{\partial x}\right)^2 + \frac{1}{\mu_r}\left(\frac{\partial \Phi}{\partial y}\right)^2 - k_0^2\ \varepsilon_r \Phi^2] d\Omega + \int_{\Gamma_{oi}} \Phi \psi d\Gamma \tag{12}$$

where Ω_{oi} and Γ_{oi} are the interior domains and boundaries of the i th subdomain respectively, o denotes the subdomain of the target. Scattered fields in the subdomains Ω_{o1}, Ω_{o2} $\cdots$, $\Omega_{o(n-1)}$, and Ω_{on} can be calculated by the finite element method.

3. Numerical Results and Discussion

In this section, numerical results are presented for two objects buried beneath the rough ground. The truncated length of the rough ground is $L_{rs} = 25.6\lambda$. A carefully tapered incident beam with $g = L_{rs}/4$ is used for excitation to eliminate the effects of the artificial edges of the modeled ground. The ground surface is characterized with Gaussian statistics, whose power spectrum function $S(k)$ can be written as

$$S(k) = \frac{\delta^2 l}{2\sqrt{\pi}} \exp(-k^2 l^2 / 4) \tag{13}$$

where δ denotes the root mean square, l represents the correlation length.

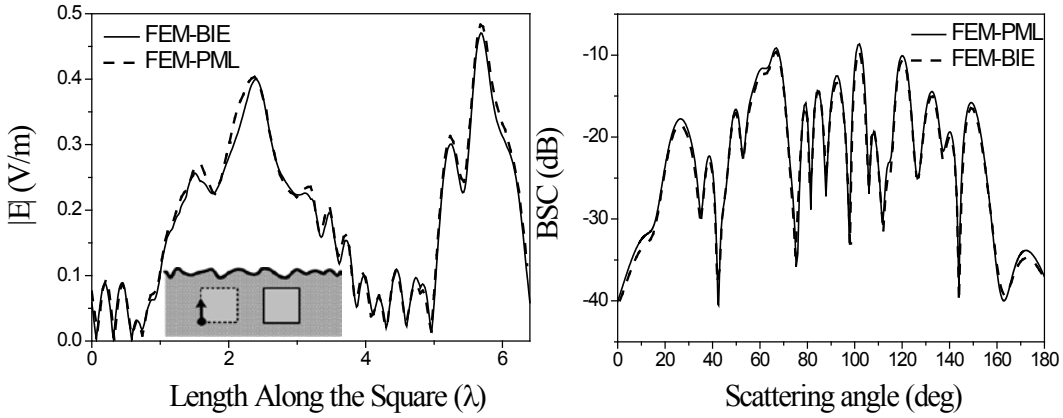

Figure 2. Scattering from two dielectric square cylinders buried under a Gaussian rough ground: (a) the absolute value of the field; (b) BSC

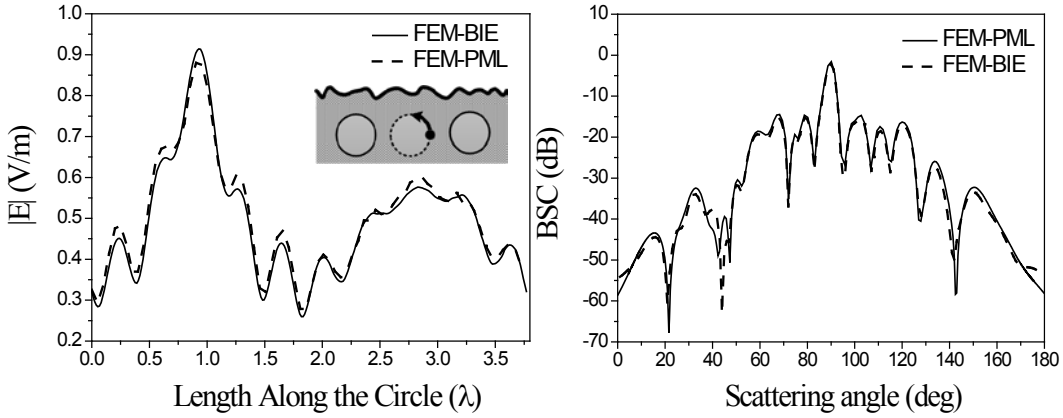

Figure 3. Scattering from three dielectric circular cylinders buried under a Gaussian rough ground: (a) the absolute value of the field; (b) BSC

In Figure 2 (a), (b) ,and (c), the FEM-BIE computer code is compared with FEM-PML. We considered two square cylinder buried under the ground. The relative dielectric constant of the ground is assumed to be $\varepsilon_r = 2.5 - j0.18$. The square cylinder of a length $l_s = 1.6\lambda$ buried at $d = 2.5\lambda$ beneath the Gaussian rough surface. The centers of two square cylinder are $x = 2\lambda$, $y = -2.5\lambda$ and $x = -2\lambda$, $y = -2.5\lambda$. The relative permittivity of two objects are $\varepsilon_r = 5.5 - j0.15$. Incident angle of the waves is set as $\theta_{inc} = 75^\circ$. The ground roughness parameters are set as $\delta = 0.15\lambda$ and $l = 0.6\lambda$. The distribution of the total electric field on a square cylinder is plotted in Figure 2 (a), and BSC of two

dielectric objects buried under the ground is shown in Figure 2 (b). It can be seen from Figure 2 (a) and (b) that two method agree with each other very well..

Considering three circular cylinders buried under the Gaussian rough surface in Figure 3, three cylinders of radius $r = 0.6\lambda$ are located at depth $d = 1.5\lambda$ under the ground surface. The relative dielectric constant of the ground is assumed to be $\varepsilon_r = 2.5 - j0.18$. Two objects are located at $(2.5\lambda, -1.5\lambda)$, $(0, -1.5\lambda)$ and $(-2.5\lambda, -1.5\lambda)$. All of objects are assumed to have the same material ($\varepsilon_r = 3.5 - j0.05$). The tapered incident wave impinges the model with an incident angle $\theta_{inc} = 90^\circ$. The root mean square of the rough ground is $\delta = 0.05\lambda$, and the correlation length is $l = 0.8\lambda$. Figure 3 shows numerical comparisons of the total electric field and BSC between different methods. The well matched results in two simulations guarantee a feasibility of the hybrid FEM-BIE again.

4. Conclusion

In this work, an efficient hybrid method combining FEM with BIE is developed, and the scattering from multiple objects buried beneath a rough surface is investigated. Compared with the published papers based on FEM employing ABC or PML, there is no need to fully enclose the scattering geometry in hybrid FEM-BIE to truncate the solution region. In our hybrid method, only the dielectric target need to be dealt with FEM, while BIE is applied to analyze the scattering from the rough surface. The interactions between the object and rough surface are taken into account by boundary integral equations. The scattering properties of two different objects buried under the ground is discussed in detail based on hybrid method. If combining FEM-BIE with the parallel technology or the optimization of the sparse matrix storage method, the hybrid method can be expected to get a more efficient result. In the future, most work will be focused on the application of hybrid FEM-BIE for a three-dimensional (3D) scattering problem and the accelerated treatment on the hybrid method.

5. Acknowledgments

This work was supported by the National Science Foundation for Distinguished Young Scholars of China under Grant number 61225002; and Fundamental Research Funds for the Central Universities under Grant number K50510070001.

6. References

1. M. M. Botha, and D. B. Davidson, “Rigorous, auxiliary variable-based implementation of a second-order ABC for the vector FEM,” *IEEE Transactions on Antennas and Propagation*, vol. 54, 2006, pp. 3499-3504.

2. L. E. R. Petersson, and J.-M. Jin, “Analysis of periodic structures via a time-domain finite-element formulation with a floquet ABC,” *IEEE Transactions on Antennas and Propagation*, vol. 54, 2006, pp. 933-944.

3. P. Liu, and Y.-Q. Jin, “Numerical simulation of bistatic scattering from a target at low altitude above rough sea surface under an EM-wave incidence at low grazing angle by using the finite element method,” *IEEE Transactions on Antennas and Propagation*, vol. 52, 2004, pp. 1205-1210.

4. E. J. Alles, and K. W. A. Van Dongen, “Perfectly matched layers for frequency-domain integral equation acoustic scattering problems,” *IEEE Transactions on Ultrasonics, Ferroelectrics, and Frequency Control*, vol. 58, 2011, pp. 1077-1086.

5. Y. Ji, and T. H. Hubing, “On the interior resonance problem when applying a hybrid FEM/MoM approach to model printed circuit boards,” *IEEE Transactions on Electromagnetic Compatibility*, vol. 44, 2002, pp. 318-323.

6. B. Alavikia, and O. M. Ramahi, “Electromagnetic scattering from cylindrical objects above a conductive surface using a hybrid finite element - surface integral equation method,” *Journal of the Optical Society of America A: Optics and Image Science, and Vision*, vol. 28, 2011, pp. 2510-2518.

7. E. I. Thorsos, “The validity of the Kirchhoff approximation for rough surface scattering using a Gaussian roughness spectrum,” *J. Acous. Soc. Am.* Vol. 83, 1988, pp. 78-92.

8. J. M. Jin, *The Finite Element Method in Electromagnetics*. New York: John Wiley, 2002.